IEEE Photonics Journal
An IEEE Photonics Society Publication

Switchable Polarization Selective Terahertz Wavefront Manipulation in a Graphene Metasurface

Volume 11, Number 3, June 2019

Yuhui Zhang
Jianxing Zhao
Jianhong Zhou
Zhiying Liu
Yuegang Fu

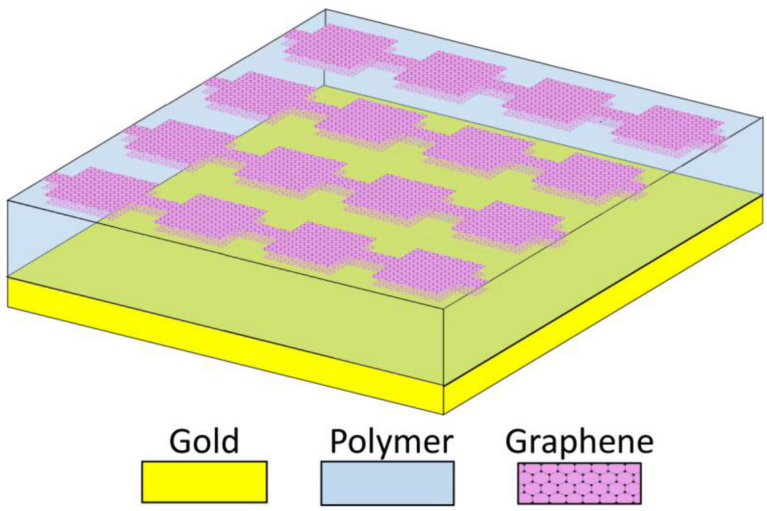

DOI: 10.1109/JPHOT.2019.2914932
1943-0655 © 2019 IEEE

Switchable Polarization Selective Terahertz Wavefront Manipulation in a Graphene Metasurface

Yuhui Zhang,[1] Jianxing Zhao,[1] Jianhong Zhou,[1,2,3] Zhiying Liu,[1,2,3] and Yuegang Fu [1,2,3]

[1]School of Optoelectric Engineering, Changchun University of Science and Technology, Changchun 130022, China
[2]Key Laboratory of Optoelectronic Measurement and Optical Information Transmission Technology of Ministry of Education, Changchun University of Science and Technology, Changchun 130022, China
[3]Key Laboratory of Advanced Optical System Design and Manufacturing Technology of the Universities of Jilin Province, Changchun 130022, China

DOI:10.1109/JPHOT.2019.2914932

Manuscript received April 10, 2019; accepted April 30, 2019. Date of current version May 30, 2019. This work was supported in part by the National Natural Science Foundation of China (NSFC) (11474041), in part by the National Natural Science Foundation of China (NSFC) (61805025), and in part by "111" Project of China (D17017). Corresponding author: Yuegang Fu (e-mail: fuyg@cust.edu.cn).

Abstract: We propose a graphene-based metasurface to investigate the function of switchable polarization selective wave manipulation in THz regime by using the finite-difference time-domain method. The proposed metasurface consists of two layers of graphene arrays, polymer dielectric spacer and a gold mirror film, which can be switched between two states by simply biasing the two graphene layers ON and OFF with the designed voltage and zero voltage without reconfiguring the Fermi energy distribution. One state is for *x* polarized wave manipulation and the other is for *y* polarization incidence. Then, the functions of switchable polarization selective anomalous reflection and focusing effect for 6 THz wave are realized by configuring the structure with specific values of Fermi energy. Moreover, we also designed the structure to focus at other spatial positions and another working frequency of 5.5 THz by reconfiguring the Fermi energy distributions.

Index Terms: Switchable graphene metasurface, polarization selection, anomalous reflection, focusing.

1. Introduction

In recent years, metasurfaces have attracted great attentions in the scientific communities. By adjusting the geometrical parameters of plasmonic antennas of metasurface, we can control the transmitted or reflected wavefront flexibly [1]–[3]. Since Capasso *et al.* first investigated beam steering in 2011 [4], many kinds of models have been reported on planar metasurfaces to achieve the functions of focusing lens [5]–[7] and anomalous reflection and refraction [8]. However, the resonator is usually selected as metal or dielectric [9]–[11], lacking active manipulation once fabricated.

Graphene, a two-dimensional material with a monolayer carbon atoms arranging in a hexagonal lattice, can support THz surface plasmons as well. The optical property of graphene is characterized by surface conductivity, which can be tuned by changing its Fermi energy via chemical doping and gate voltage [12]–[14]. Graphene based metaface can also be designed to manipulate wave in THz

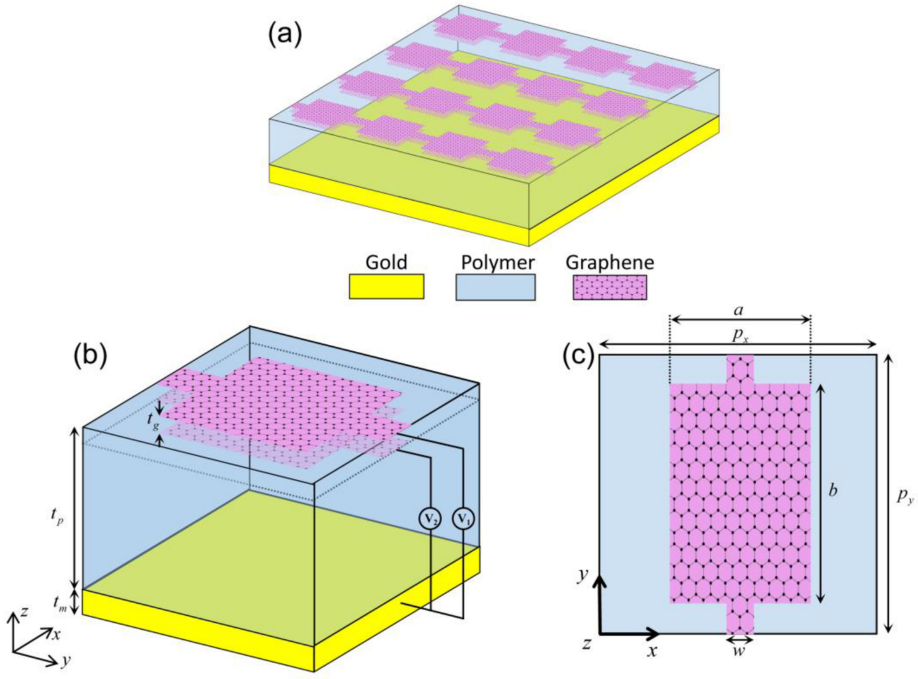

Fig. 1. Schematic diagram of the proposed graphene metasurface. (a) The fragment of the proposed graphene metasurface. (b) The unit cell of the proposed metasurface. (c) Top view of the unit cell.

frequency region [15]–[17]. Recently, graphene ribbons are introduced to metasurface to design cylindrical lens [18], [19], in which only one polarization incidence is considered, and the switchable characteristic of graphene has not been fully investigated.

In this paper, we have reported the numerical investigation of the switchable polarization selective terahertz wavefront manipulation in a graphene metasurface by using the finite-difference time-domain (FDTD) method. The proposed graphene metasurface consists of two layers of graphene arrays, polymer dielectric spacer and a gold mirror film, which can be switched between two states by simply turning ON and OFF the two graphene layers without reconfiguring the Fermi energy distribution, i.e., one graphene layer is biased to the designed values while the other is at zero bias. Among the two working states, one is for x polarized wave manipulation and the other is for y polarization. First, we periodically arranged thirty unit with a phase difference of 12°, both the state 1 for x polarization incidence and state 2 for y polarization incidence can achieve 25° reflection angle at 6 THz normal incident wave. Then we designed a cylindrical lens with a focal length of $F = 200\ \mu$m, the performance of the proposed structure is in good agreement with the analysis result. We also show the cases of state 1 with y-polarization incidence and state 2 with x-polarization incidence, no anomalous reflection and focusing effect occurs. Thus switchable polarization selective terahertz wave manipulation is achieved by switching the designed structure between the states 1 and 2. Moreover, we also design the structure to focus at different spatial positions and working frequencies by reconfiguring the Fermi energy distributions. We believe that the proposed structure can provide an improved method of terahertz wave manipulation.

2. Structure Design

Figure 1(a) shows the fragment of the proposed graphene metasurface. Two identical layers of continuous graphene array stack on the top, which can be separately modulated to different Fermi energy by changing the gate voltages as shown in Fig. 1(b). A gold film acting as a perfect reflector is on the bottom of the structure. Thus, a Fabry-Perot resonator is formed to enhance the interaction

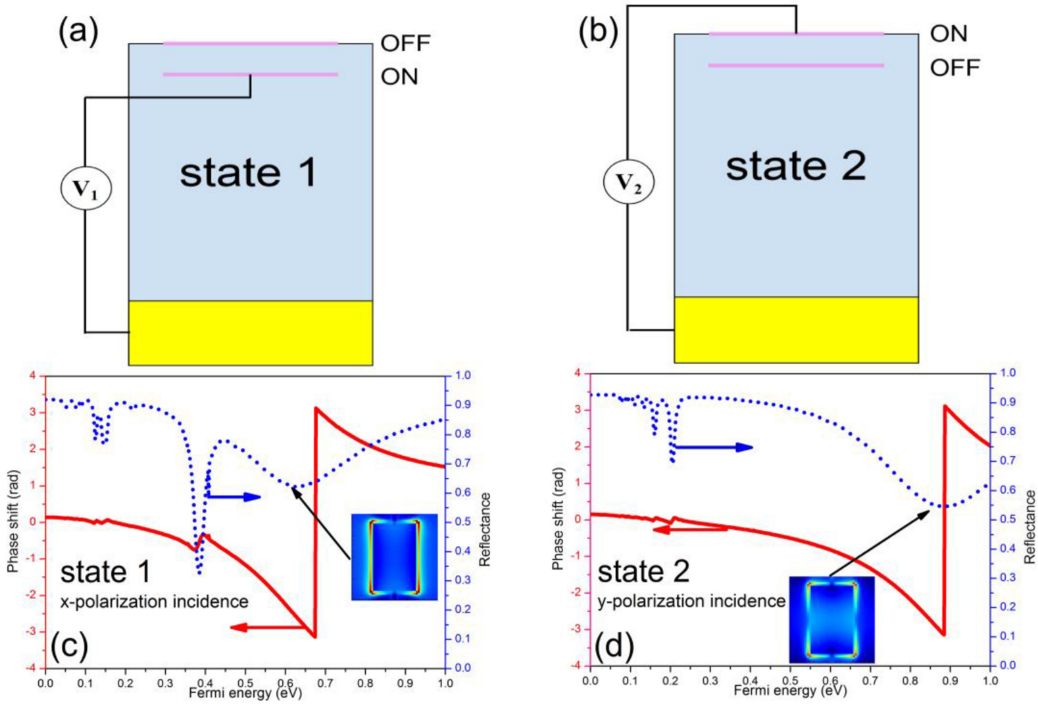

Fig. 2. (a) Cross section view of state 1 with the only bottom graphene works. (b) Cross section view of state 2 with the only top graphene works. Phase shift and reflectance of reflected wave of (c) state 1 with x polarization incidence and (d) state 2 with y polarization incidence.

between THz wave and graphene and to expand the phase range [20]. The dielectric spacer is chosen as polymer with a refractive index of 1.53, due to its low loss and stable refraction index for THz wave [21]. The monolayer graphene is characterized by surface conductivity, which can be simplified in THz frequency to a Drude-like expression [18]:

$$\sigma_g = \frac{e^2 E_f}{\pi \hbar^2} \frac{i}{\omega + i\tau^{-1}} \tag{1}$$

where ω is the working radian frequency, e is electron charge, $\hbar$ is reduced Planck's constant, E_f is the Fermi energy, and τ is the electron-photon relaxation time. In our study, τ is assumed to be 10^{12} s [22]. The Fermi energy of graphene can be tuned within the range from 0 to 1 eV via voltage control [23], resulting in a 2π phase shift range for the reflected wave. The geometric parameters of the structure shown in Figs. 1(b) and 1(c) are $t_g = 1$ μm, $t_p = 8$ μm, $t_m = 2$ μm, $p_x = p_y = 4$ μm, $a = 2$ μm, $b = 3.2$ μm and $w = 0.2$ μm. To numerically investigate the wave manipulating performance of the proposed graphene metasurface, finite-difference time-domain (Lumerical FDTD solutions) software is used to calculate the phase shift and propagation characteristics of incident THz waves.

3. Results and Discussion

To realize switchable polarization selective THz wave manipulation, we design the structure with two working states by separately turning ON and OFF the two graphene layers. In state 1, as shown in Fig. 2(a), only the bottom graphene layer works while the top graphene layer is at zero bias, i.e., the Fermi energy of the top graphene layer is kept 0 eV, resulting in a near zero value of conductivity [24], and the bottom graphene layer is biased with the designed gate voltage to manipulate the incident wave. And in state 2, only the top graphene layer is biased as shown in Fig. 2(b). Then we design the bottom graphene layer of state 1 to manipulate x polarized incident

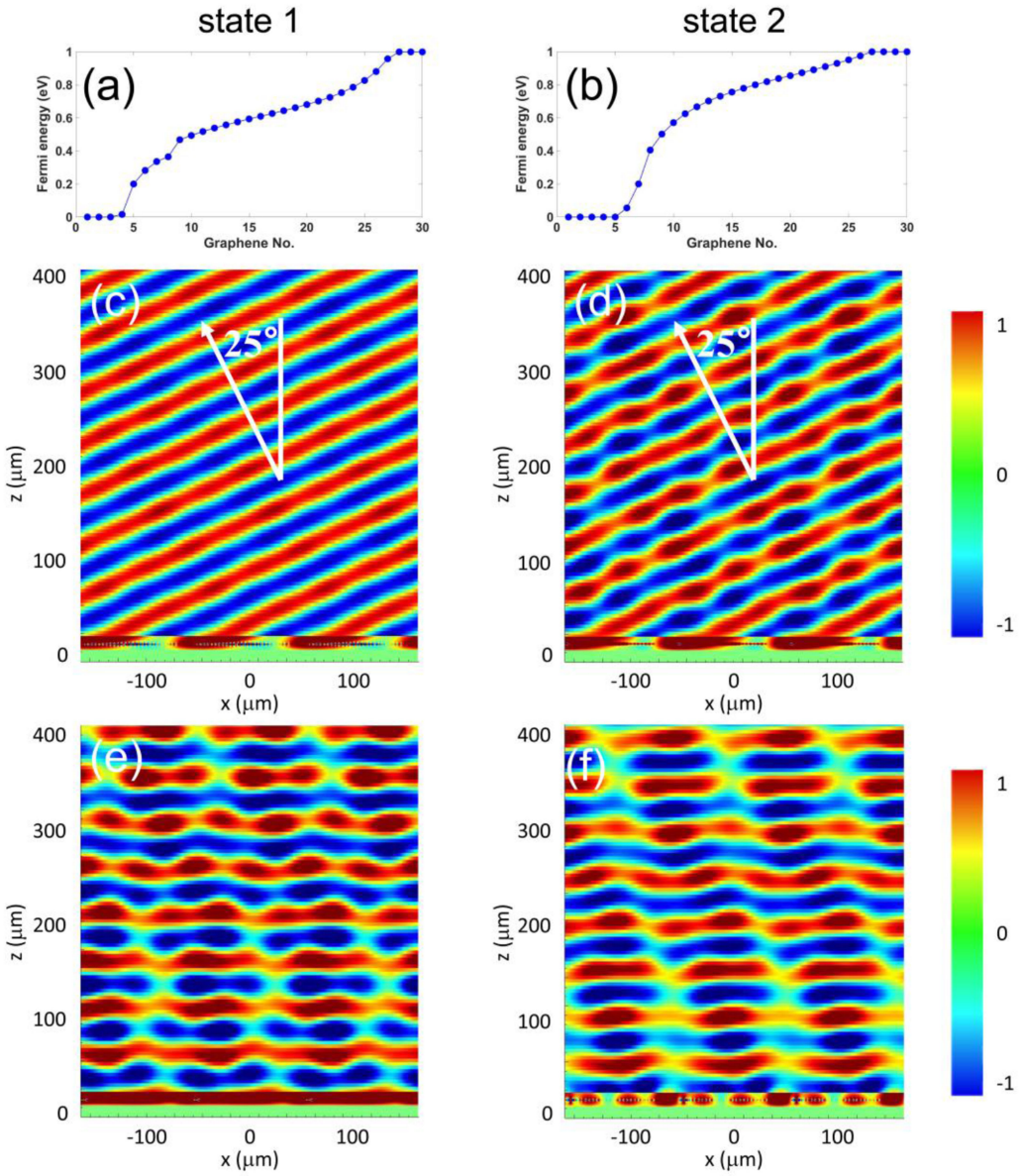

Fig. 3. The Fermi energy distribution of the (a) bottom graphene array of state 1 and (b) top graphene array of state 2 (c) Reflected electric field Ex distribution of state 1 with x polarization incidence. (d) Reflected electric field Ey distribution of state 2 with y polarization incidence. The working frequency is 5 THz. (e) Ey distribution of state 1 with y polarization incidence. (f) Ex distribution of state 2 with x polarization incidence.

wave and the top graphene layer of state 2 to manipulate y polarized incident wave. By switching the designed structure between the states 1 and 2, the switchable polarization selective terahertz wave manipulation is achieved. We choose the working frequency of 6 THz in both states. In order to separately control the x and y polarized wave, we design the structure to resonant at different Fermi energies in each state by adjusting the geometric parameters of the graphene. The resonance dip of state 1 for x polarization incidence is around 0.6 eV, and that of state 2 is around 0.9 eV. The corresponding phase shift and reflectance of states 1 and 2 are shown in Figs. 2(c) and 2(d), respectively. Near 2π phase shift can be acquired in both states. The insets show the electric field distributions of the resonant modes, which are electric dipoles to control the amplitude and phase

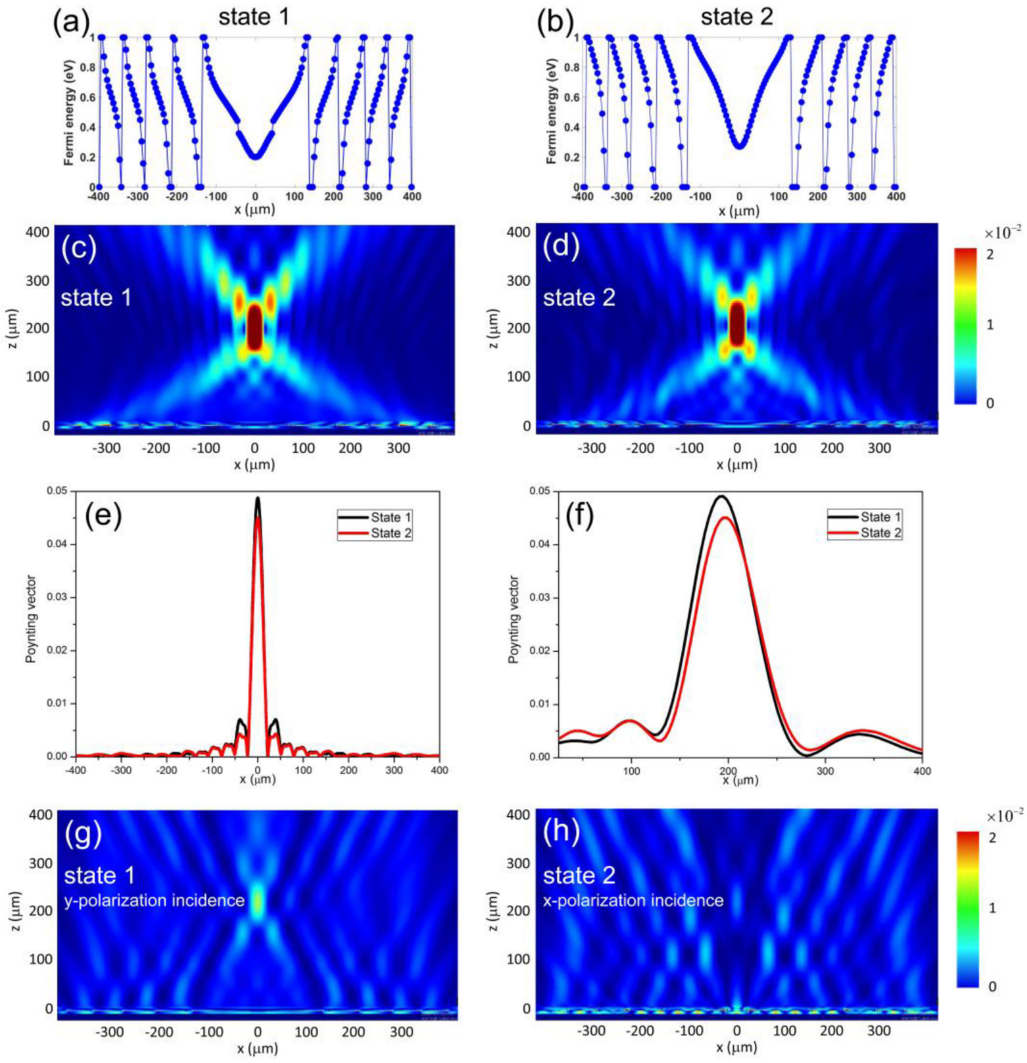

Fig. 4. The Fermi energy distributions of (a) bottom graphene array of state 1 and (b) top graphene array of state 2. The simulated Poynting vector of the metalens for (c) state 1 with x-polarization incidence, (d) state 2 with y-polarization incidence, (e) state 1 with y-polarization incidence and (f) state 2 with x-polarization incidence at the working frequency of 6 THz. The intensity distributions of the two states along the (g) x direction and (h) z direction.

of the reflected wave. Therefore, by switching from one state to another, the proposed structure can realize the polarization selective THz wave manipulation.

In metasurface, light manipulation can be realized by introducing a phase gradient of $d\varphi/dx$ along the interface of metasurface, which can be characterized by the generalized Snell's law [4]. The reflection angle for normal incidence can be calculated by the expression

$$\sin(\theta_r) = \frac{\lambda_0}{2\pi n_i}\frac{d\varphi}{dx} \tag{2}$$

where φ is the phase shift, x is the length of metasurface, λ_0 is the incident wavelength and n_i is the refractive index of the material at the incident side. In our case, n_i is set as 1. For state 1, we select thirty continuous graphene units with different values of Fermi energy from Fig. 2(c) to cover the full 2π phase shift for x polarized incident wave, then the phase shift between two adjacent unit is 12°. Based on Eq. (2), the reflection angle is then calculated to be 30°. The Fermi energy

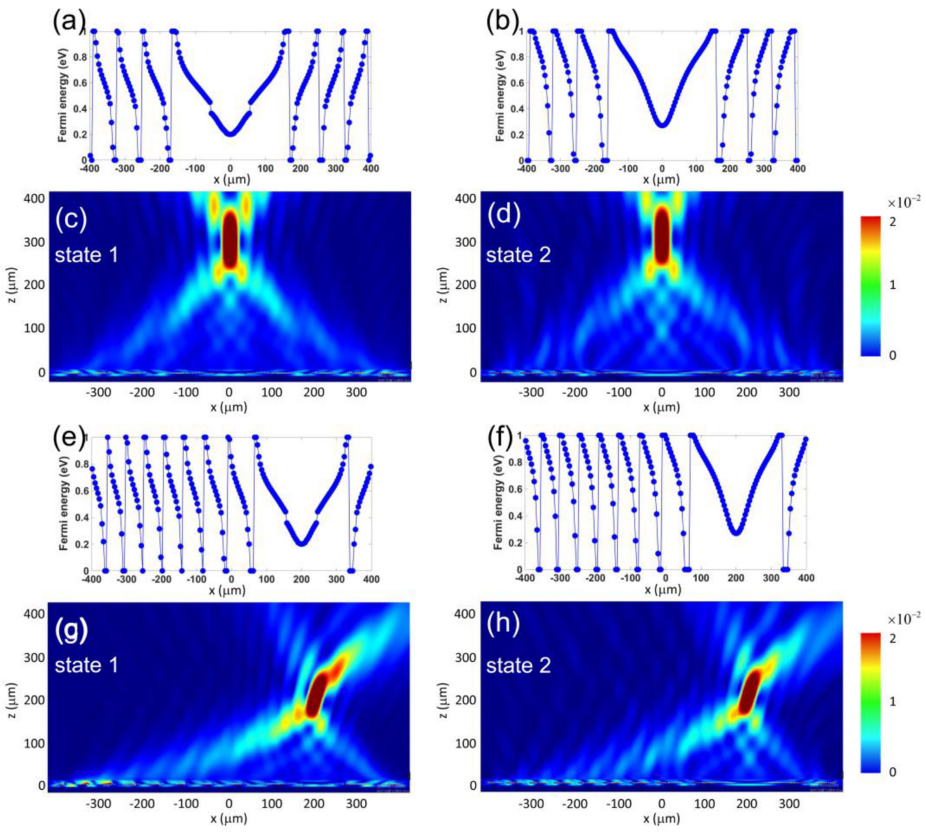

Fig. 5. The Fermi energy distributions of the designed metalens for (a) state 1 and (b) state 2 of the focal point position of [$x = 0,\ z = 300\ \mu$m], and (e) state 1 and (f) state 2 of the focal point position of [$x = 100,\ z = 200\ \mu$m]. The simulated Poynting vector of the metalens for (c) state 1 and (d) state 2 of the focal point position of [$x = 0,\ z = 300\ \mu$m], and (g) state 1 and (h) state 2 of the focal point position of [$x = 100,\ z = 200\ \mu$m].

distribution of the bottom graphene structures in a super-cell is shown in Fig. 3(a). Note that the phase shift produced by Fermi energy shown in Fig. 2(c) cannot cover the whole 2π range, and the Fermi energy values out of range are replaced by 0 or 1 eV as approximations, which causes small discrepancies between the designed values and the actual results. The x component electric field distribution of the reflected wave is shown in Fig. 3(c), in which a smaller reflection angle of 25° than the theoretical expectation is acquired due to the approximation in the designing process. Then we switch the structure to state 2. For y polarized incident wave, we also select thirty continuous units from Fig. 2(d) with a phase difference of 12°. The Fermi energy distribution of the top graphene structures is shown in Fig. 3(b). The y component electric field distribution is shown in Fig. 3(b), which performs a 25° reflection angle as well. In order to validate the polarization selective wave manipulation effect, we also show the results of state 1 with y-polarization incidence and state 2 with x-polarization incidence. The y and x components electric field distributions are shown in Figs. 3(e) and 3(f), from which we can see that no anomalous reflection effect occurs. Therefore, the state 1 manipulates x polarized wave only, while the state 2 manipulates y polarized wave only.

The proposed structure can be designed to achieve the function of cylindrical lens. To achieve focusing effect, the relative phase of reflected wave at position x from the center should follow the expression

$$\varphi(x) = \frac{2\pi}{\lambda_0}\left(\sqrt{(x+\Delta x)^2 + F^2} - F\right) \tag{3}$$

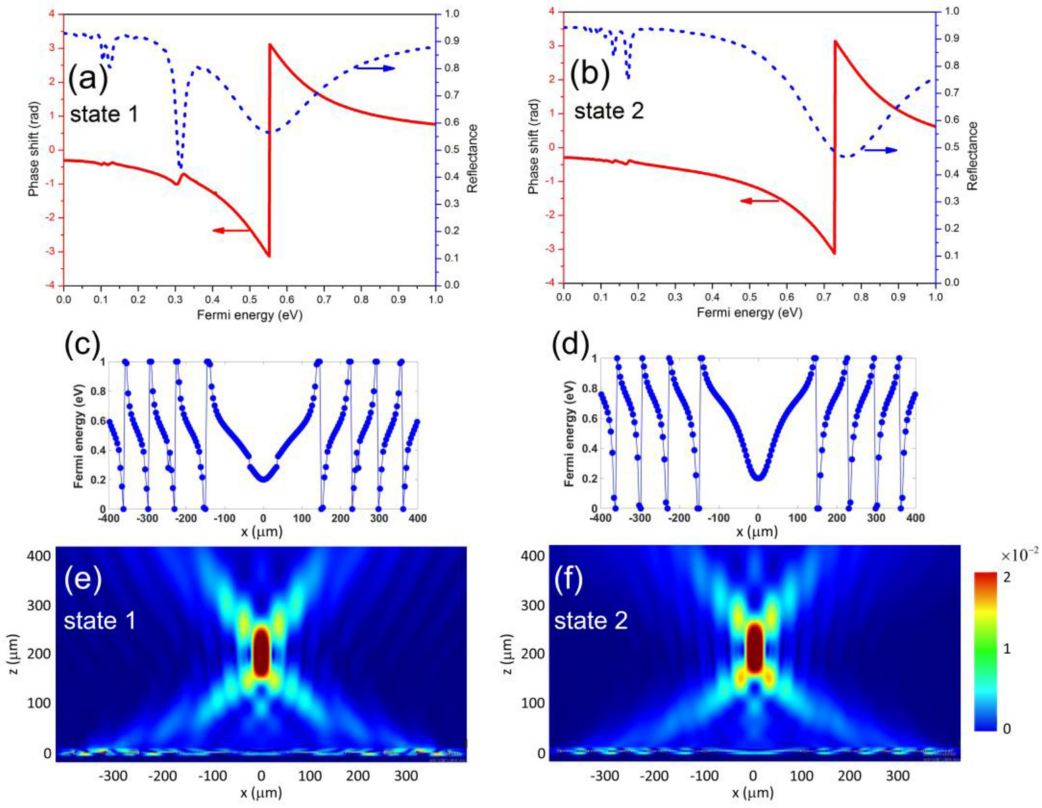

Fig. 6. Phase shift and reflectance of reflected wave of (a) state 1 with x polarization incidence and (b) state 2 with y polarization incidence at the working frequency of 5.5 THz. The designed Fermi energy distributions of states 1 and 2 are shown in Figs. 5(c) and 5(d) at the working frequency of 5.5 THz. The simulated Poynting vector of the metalens for (e) state 1 with x polarized incidence and (f) state 2 with y polarized incidence at the working frequency of 5.5 THz.

where λ_0 is incident wavelength, F represents the designed focal length and Δx represents the shift of focal point along x axis. We choose the center Fermi energy as 0.2 eV. Based on Figs. 2(c) and 2(d), we design a switchable polarization selective metalens with the focal length of $F = 200\ \mu$m, and $\Delta x = 0$. The width of the metalens is designed as 800 μm. The designed metalens can achieve polarization selective focusing of the 6THz incident wave when switched between the two working states. The Fermi energy distributions of state 1 and state 2 are shown in Figs. 4(a) and 4(b). Based on such Fermi energy distributions, we simulate the cylindrical lens and the simulated results of state 1 for x-polarization incidence and state 2 for y-polarization incidence are shown in Figs. 4(c) and 4(d), respectively. The focal lengths of state 1 and state 2 are 194 μm and 197 μm, which agree well with the designed values. Fig. 4(g) shows the Poynting vector distributions along x direction, from which we can see that the values of full width at half maximum (FWHM) of state 1 and state 2 are 25.5 μm and 26 μm, respectively. And that of state 1 and state 2 along z direction are shown in Fig. 4(d), the FWHM of state 1 and state 2 are 73.3 μm and 71.5 μm, respectively. The results of state 1 with y-polarization incidence and state 2 with x-polarization incidence are also shown in Figs. 4(e) and 4(f), which are not convincing for focusing devices. Thus, the state 1 focuses x polarized incident wave only and state 2 focuses y polarized wave only. A switchable polarization selective cylindrical lens is achieved by switching the structure between states 1 and 2.

Furthermore, the switchable metalens can also be designed to focus at other spatial positions. Thus, based on the results analyzed above, a metalens with the focal length of $F = 300\ \mu$m is designed, i.e., [$x = 0,\ z = 300\ \mu$m]. The designed Fermi energy distributions of states 1 and 2 are shown in Figs. 5(a) and 5(b), and the simulated intensity distributions for two states are shown in

Figs. 5(c) and 5(d) with the focal lengths of 290 μm and 297 μm, respectively. We also design a switchable metalens with a focal point position of [$x = 100$, $z = 200$ μm], and the designed Fermi energy distributions of states 1 and 2 are shown in Figs. 5(e) and 5(f) the simulated results of the two states are shown in Figs. 5(g) and 5(h). Moreover, the proposed metalens can also be designed to work at other frequencies. Then we select the working frequency of 5.5 THz. The phase shift and reflectance of states 1 and 2 are shown in Figs. 6(a) and 6(b). Based on Figs. 6(a) and 6(b), we design the switchable metalens working at the frequency of 5.5 THz, and the Fermi energy distributions for states 1 and 2 are shown in Figs. 6(c) and 6(d). The simulated results of its two states are shown in Figs. 6(c) and 6(d), the focal lengths of the two states are 290 μm and 295 μm, respectively.

4. Conclusion

In summary, we have numerically investigated the switchable polarization selective terahertz wave manipulation effect in a graphene metasurface by using FDTD method. By voltage control, the proposed graphene metasurface can be switched between two states by simply turning ON and OFF the two graphene layers without reconfiguring the Fermi energy distribution, i.e., one graphene layer is biased to the designed values while the other layer is at zero bias. Among the two working states, one is for x polarized wave manipulation and the other is for y polarization. By introducing a phase gradient along the interface of the metasurface, the anomalous reflection effect can be achieved in both state1 and state 2. Then a cylindrical lens with a focal length of $F = 200$ μm was designed, and the performance of both states 1 and 2 of the proposed structure is in good agreement with the analysis result. The cases that state 1 with x-polarization incidence and state 2 with y polarization incidence are also investigated, which perform no wave manipulation effect. Therefore, by switching between the two states, the structure can achieve the function of switchable polarization selectively terahertz wave manipulation. Moreover, the structure can also be designed to focus at different spatial positions and working frequencies. Our findings are beneficial in developing new methods of terahertz wave manipulation.

References

[1] H. T. Chen, A. J. Taylor, and N. Yu, "A review of metasurfaces: Physics and applications," *Rep. Prog. Phys.*, vol. 79, 2016, Art. no. 076401.

[2] L. Zhang, S. T. Mei, K. Huang, and C. W. Qiu, "Advances in full control of electromagnetic waves withmetasurfaces," *Adv. Opt. Mater.*, vol. 4, pp. 818–833, 2016.

[3] V. C. Su, C. H. Chu, G. Sun, and D. P. Tsai, "Advances in optical metasurfaces: Fabrication and applications [Invited]," *Opt. Exp.*, vol. 26, pp. 13148–13182, 2018.

[4] N. Yu *et al.*, "Light propagation with phase discontinuities: Generalized laws of reflection and refraction," *Science*, vol. 334, pp. 333–337, 2011.

[5] R. Li *et al.*, "Arbitrary focusing lens by holographic metasurface," *Photon. Res.*, vol. 3, pp. 252–255, 2015.

[6] A. Pors, M. G. Nielsen, R. L. Eriksen, and S. I. Bozhevolnyi, "Broadband focusing flat mirrors based on plasmonic gradient metasurfaces," *Nano Lett.*, vol. 13, pp. 829–834, 2013.

[7] D. Y. Lu *et al.*, "Broadband reflective lens in visible bandbased on aluminum plasmonic metasurface," *Opt. Exp.*, vol. 26, pp. 34956–34964, 2018.

[8] X. Ni, N. K. Emani, A. V. Kildishev, A. Boltasseva, and V. M. Shalaev, "Broadband light bending with plasmonic nanoantennas," *Science*, vol. 335, pp. 427–427, 2012.

[9] M. Khorasaninejad and F. Capasso, "Metalenses: Versatile multifunctional photonic components," *Science*, vol. 358, 2017, Art. no. 8100.

[10] P. Lalanne and P. Chavel, "Metalenses at visible wavelengths: Past, present, perspectives," *Laser Photon. Rev.*, vol. 11, 2017, Art. no. 1600295.

[11] P. Genevet, F. Capasso, F. Aieta, M. Khorasaninejad, and R. Devlin, "Recent advances in planar optics: From plasmonic to dielectric metasurfaces," *Optica*, vol. 4, pp. 139–152, 2017.

[12] A. Vakil and N. Engheta, "Transformation optics using graphene," *Science*, vol. 332, pp. 1291–1294, 2011.

[13] F. H. L. Koppens, D. E. Chang, and F. J. G. D. Abajo, "Graphene plasmonics: A platform for strong light–matter interactions," *Nano Lett.*, vol. 11, pp. 3370–3377, 2011.

[14] L. Jum *et al.*, "Graphene plasmonics for tunable terahertz metamaterials," *Nature Nanotechnol.*, vol. 6, pp. 630–634, 2011.

[15] Z. Liu and B. Bai, "Ultra-thin and high-efficiency graphene metasurface for tunable terahertz wave manipulation," *Opt. Exp.*, vol. 25, pp. 8584–8592, 2017.

[16] P. Ding, Y. Li, L. Shao, X. Tian, J. Wang, and C. Fan, "Graphene aperture-based metalens for dynamic focusing of terahertz waves," *Opt. Exp.*, vol. 26, pp. 28038–28050, 2018.
[17] M. Hashemi, A. Moazami, M. Naserpour, and C. J. Zapata-Rodriguez, "A broadband multifocal metalens in the terahertz frequency range," *Opt. Commun.*, vol. 370, pp. 306–310, 2016.
[18] T. Yatooshi, A. Ishikawa, and K. Tsuruta, "Terahertz wavefront control by tunable metasurface made of graphene ribbons," *Appl. Phys. Lett.*, vol. 107, 2015, Art. no. 053105.
[19] W. Ma, Z. Huang, X. Bai, P. Zhan, and Y. Liu, "Dual-band light focusing using stacked graphene metasurfaces," *ACS Photon.*, vol. 4, pp. 1770–1775, 2017.
[20] G. Zheng, H. Muhlenberne, M. Kenney, G. Li, T. Zentgraf, and S. Zhang, "Metasurface holograms reaching 80% efficiency," *Nature Nanotechnol.*, vol. 10, pp. 308–312, 2015.
[21] P. D. Cunningham *et al.*, "Broadband terahertz characterization of the refractive index and absorption of some important polymeric and organic electro-optic materials," *J. Appl. Phys.*, vol. 109, 2011, Art. no. 043505.
[22] W. Gao, J. Shu, C. Qiu, and Q. Xu, "Excitation of plasmonic waves in graphene by guided-mode resonances," *ACS Nano*, vol. 6, pp. 7806–7813, 2012.
[23] J. S. Gomez-Diaz and J. Perruisseau-Carrier, "Graphene-based plasmonic switches at near infrared frequencies," *Opt. Exp.*, vol. 21, pp. 15490–15504, 2013.
[24] Y. Zhang, Y. J. Feng, T. Jiang, J. Cao, J. M. Zhao, and B. Zhu, "Tunable broadband polarization rotator in terahertz frequency based on graphene metamaterial," *Carbon*, vol. 133, pp. 170–175, 2018.